Beesley, J., Baum, H., Hodgson, L., Verkade, P., Banting, G., & Woolfson, D. (2018). Modifying self-assembled peptide cages to control internalization into mammalian cells. *Nano Letters*. https://doi.org/10.1021/acs.nanolett.8b02633

Modifying Self-Assembled Peptide Cages to Control Internalization into Mammalian Cells

Joseph L. Beesley,[†,‡] Holly E. Baum,[§,⊥,‡] Lorna R. Hodgson,[§] Paul Verkade,[§,ǀ,⊥] George S. Banting,*[,§] and Derek N. Woolfson*[,†,§,⊥]

[†]School of Chemistry, University of Bristol, Bristol BS8 1TS, United Kingdom

[§]School of Biochemistry, University of Bristol, Bristol BS8 1TD, United Kingdom

[ǀ]Wolfson Bioimaging Facility, University of Bristol, Bristol BS8 1TD, United Kingdom

[⊥]BrisSynBio, University of Bristol, Bristol BS8 1TQ, United Kingdom

Supporting Information Placeholder

ABSTRACT: Nanoparticles can be used to transport a variety of biological cargoes into eukaryotic cells. Polypeptides provide a versatile material for constructing such systems. Previously, we have assembled nanoscale peptide cages (SAGEs) from *de novo* designed coiled-coil modules. Here, we show that the modules can be extended with short charged peptides to alter endocytosis of the assembled SAGE particles by cultured human cells in a tunable fashion. First, we find that the peptide extensions affect coiled-coil stability predictably: *N*-terminal polylysine and *C*-terminal polyglutamate tags are destabilizing; whereas, the reversed arrangements have little impact. Second, the cationic assembled particles are internalized faster and to greater extents by cells than the parent SAGEs. By contrast, anionic decorations markedly inhibit both aspects of uptake. These studies highlight how the modular SAGE system facilitates rational peptide design to fine-tune the bioactivity of nanoparticles, which should allow engineering of tailored cell-delivery vehicles.

Keywords: de novo *peptide, coiled coil, self-assembly, nanoparticle, cellular internalization*

A wide variety of nanoparticles have been shown to be internalized by eukaryotic cells. These range from hard inorganic nanoparticles, through polymer-based systems, to self-assembled peptide- and protein-based cages.[1] Such nanoparticles have been developed for various applications at the biointerface, particularly for the delivery of therapeutic and diagnostic agents.[2] Within these approaches, soft polypeptide-based nanoparticles are emerging as exciting new materials due to advances in polypeptide design and engineering, and their potential biocompatibility and monodispersity.[3] These systems can be classified into three broad categories: modified natural assemblies, including enzyme cages and viral capsids;[4] self-assembled protein cages assembled using engineered proteins;[5] and nanoparticles and cages assembled from *de novo*-designed peptides.[6] While natural systems often offer robust scaffolds for nanoparticle development, completely *de novo* cage-like assemblies have the potential to provide considerable control over biophysical properties with their improved tractability.[7] Furthermore, recent advances in computational protein design and high resolution structural techniques now allow the precise design and characterization of such assemblies.[8] Although bioactive cargo delivery to eukaryotic cells is well established with repurposed natural cages, the use of designed systems is only just being realized.[9]

Recently, we have described the design, assembly and characterization of self-assembled peptide nanocages (SAGEs) built with two components from a toolkit of *de novo* designed coiled-coil peptides.[10] Briefly, the two chains of a heterodimeric coiled coil (CC-Di-AB) are individually linked to a homotrimeric peptide (CC-Tri3) through disulfide bonds on their solvent-exposed faces (Figure 1A). Upon mixing, these "hub" peptide conjugates associate *via* the formation of the heterodimers into a hexagonal lattice that closes to yield quasi-spherical objects. Molecular dynamics simulations suggest that the SAGE lattice closes leading to presentation of the *N* termini of the CC-Tri3 peptides on the exterior face of the assembly.[10b] Coarse-grained simulations of hub association and the biomineralization of silica onto the SAGE surface provide further detail and understanding of the lattice assembly and structure.[11] In addition, the modular nature of the SAGE design has allowed the incorporation of multiple protein cargoes within particles and to different loading densities.[12] Here, we build on this work to develop SAGE particles for tunable

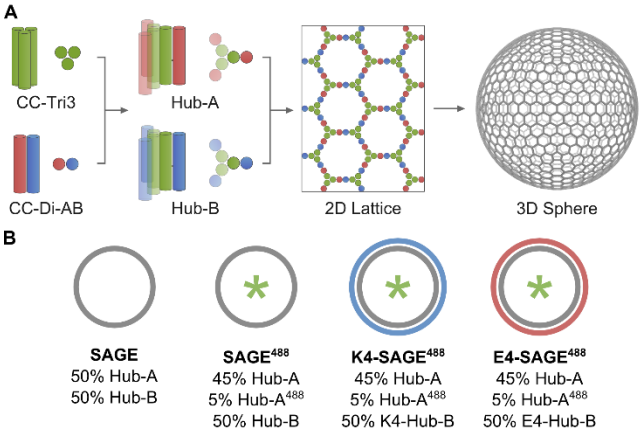

Figure 1. Schematics of SAGE assembly and example compositions. (**A**) CC-Tri3 (green) is coupled to CC-Di-A (red) and CC-Di-B (blue) to form Hub-A and Hub-B, respectively. When mixed, these peptides assemble through heterodimer association to form a hexagonal lattice that closes to form SAGE particles. (**B**) SAGE compositions employed in this study where green asterisk indicates the presence of Alexa Fluor 488 and blue and red halos represent a cationic or anionic surface charge, respectively.

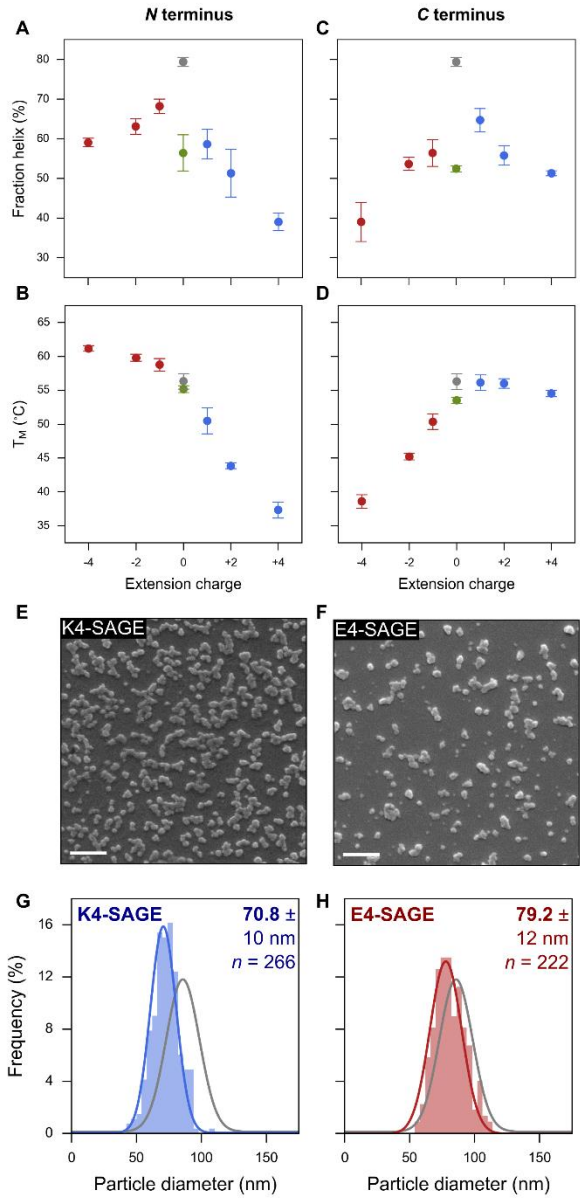

Figure 2. Biophysical characterization of SAGE components and particles. (**A** – **D**) Mono-, di- and tetrapeptide extensions of Lys (blue) and Glu (red) were introduced at the *N* (**A** & **B**) and *C* (**C** & **D**) termini of CC-Tri3. CC-Tri3 (grey), G4-CC-Tri3 (**A** & **B**; green) and CC-Tri3-G4 (**C** & **D**; green) were also analyzed. Fraction helix and T_M were determined by CD spectroscopy. Conditions: 50 μM peptide, 250 μM tris(2-carboxyethyl)phosphine (TCEP), phosphate-buffered saline (PBS). Points show statistical mean ± standard deviation ($n = 3$). (**E** – **H**) Representative scanning electron micrographs (scale bars: 500 nm) and particle sizing with Gaussian fit of K4-SAGE (**E** & **G**) and E4-SAGE (**F** & **H**). Gaussian fit of SAGE (92.0 ± 14 nm) shown in grey (**G** & **H**). Conditions: 50 μM peptide, HEPES-buffered saline (HBS).

biointerfacing through the systematic modification of their surfaces.

It is widely accepted that surface charge alters the interactions of nanoparticles with cells and their subsequent internalization.[13] To explore this concept in the SAGE system, a series of CC-Tri3 variants was synthesized bearing 1, 2 or 4 positively charged lysine (Lys) or negatively charged glutamic acid (Glu) residues at the *N* or *C* terminus (Table S1). When assembled into SAGE particles, these components should present increasing amounts of positive or negative charge at the particle exterior (*N*-terminal) or interior (*C*-terminal) according to our working model for SAGE assembly. We used solution-phase biophysical methods to characterize the CC-Tri3 variants, along with two uncharged control peptides: G4-CC-Tri3 and CC-Tri3-G4.

By circular dichroism (CD) spectroscopy, all peptides were found to be α helical at 5 °C and underwent cooperative unfolding upon heating (Figures S4 & S5). Moreover, like CC-Tri3, all of the tetrapeptide-labelled peptides were trimeric in solution by analytical ultracentrifugation (Figure S6). The fraction helix (FH) and midpoint temperature of thermal unfolding (T_M) values were extracted from the CD data and used for the following comparative analysis.

At the *N* terminus, the introduction of a control tetraglycine extension led to a loss in overall helicity, which stands to reason as the extension is expected to be unfolded (Figure 2A). The T_M was unaffected, confirming that this modification did not perturb the folded coiled-coil assembly (Figure 2B). Similarly, the addition of increasing numbers of Glu residues gave progressively lower helicities and affected the T_M minimally (Figures 2A & B); if anything, the modified peptides were slightly more stable than the parent. Again, we interpret this as the Glu extensions being largely unfolded and having little impact on the structure and stability of the core homotrimer. Interestingly, and by contrast, increasing Lys extensions markedly and proportionally reduced both the helicities and the thermal stabilities of the peptides (Figures 2A & B). The loss of helicity was more than expected for an unfolded extension, and the K4-CC-Tri3 peptide was some 20 ˚C less stable than G4-CC-Tri3.

The correlations were reversed for the analogous *C*-terminal modifications: Lys extensions of increasing length reduced peptide helicity no more than expected from the CC-Tri3-G4 control, and they perturbed the T_M only marginally (Figure 2C & D). However, additional Glu residues led to far greater decreases in helicity and thermal stability, and these were proportional to length of the extension. Interestingly, the FH and T_M values of CC-Tri3-E4 and K4-CC-Tri3 were similar; *i.e.*, both are destabilized to similar extents.

These data seem best explained as follows: the introduction of short charged peptides to the termini of monomeric α-helical peptides is known to affect helicity and stability.[14] Specifically, for such stand-alone helices, proximal anionic and cationic side chains stabilize partial positive and negative charges at the *N* and *C* termini, respectively. The switched arrangements are destabilizing. The findings presented herein extend this view to coiled coil-based peptide oligomers. Moreover, in the coiled-coil systems it appears that potential inter-helical side-chain repulsions between the extensions are tolerated, but only when the side chain-main chain interactions are favorable. We suggest that such sequence features and electrostatics interactions are taken into account when designing or engineering supramolecular polypeptide assemblies such as the SAGEs.

Next, we used the CC-Tri3 variants to construct new hubs for SAGE assembly. The *N*-terminally extended peptides were coupled to CC-Di-B to form Hub-B variants that should present the charged extensions at the external face of an assembled SAGE (Table S2). In addition, we made a variant of CC-Tri3 with a pendant Alexa Fluor 488 located near the *C* terminus to allow direct detection of SAGE particles (Table S1). This was coupled to CC-Di-A to form the fluorescently labelled hub peptide Hub-A^{488}. The introduction of the fluorophore slightly increased the stability of the CC-Tri3 peptide (Figure S8) and did not affect assembly into SAGEs (Figure S9). By combining decorated and non-decorated hub peptides, a range of SAGE compositions carrying different surface charges

and the small-molecule dye was assembled (Figure 1B & Table S3).

The impact of peptide decorations on SAGE morphology was assessed by scanning electron microscopy (SEM; Figures 2E & F & S9). All modified SAGEs had quasi-spherical morphologies similar to the parent SAGE particles, indicating that the decorations did not markedly affect SAGE assembly. However, the average particle diameters were reduced by 12 – 21 nm across the compositions compared with the parents. One possible explanation for this is that *N*-terminally displayed charged residues further promote the anticipated wedge shapes of the hubs leading to higher radii of curvature and smaller particles. This is consistent with our working model for SAGE assembly and structure.[10b]

We tested how the decorated SAGE particles interacted with mammalian cells in culture. Neither the *de novo* component peptides nor the assembled particles were cytotoxic to HeLa cells over 24 h (Figure S10). Fluorescent SAGE^{488} particles were then introduced to HeLa cells for 2 h and visualized by confocal microscopy. Fluorescence was observed within the limits of the actin cytoskeleton revealing that SAGEs had been internalized without the need for specific functionalization (Figure 3B & S11). The punctate intracellular distribution is indicative of active internalization by endocytosis and not direct penetration across the membrane, which would result in disperse fluorescence throughout the cytosol.[15] SAGE^{488} internalization was found to be completely inhibited at 4 °C and dramatically reduced at 20 °C, strongly supporting energy-dependent endocytic uptake (Figure S12). Further studies are underway to determine the specific mechanism(s) of SAGE endocytosis.

To investigate the impact of SAGE surface charge on the rate and efficiency of endocytosis, the charged Hub-B variants were used to assemble a series of fluorescent SAGEs with varying surface charges (Table S3). All particles entered the cytoplasm in a temperature-dependent manner and gave similar punctate distributions (Figure S12). However, the intracellular load was affected dramatically by surface electrostatics: positive charge gave greater accumulation and negative charge impeded uptake (Figures 3C & D & S13). Furthermore, there was a dose response for the anionic particles, with increasing negative charge lowering the intracellular load, but no response for an increasingly cationic particle surface.

Next, we quantified SAGE uptake temporally across the entire cell population using flow cytometry (Figure 3E & F). The data were analyzed in two ways (see Methods): the proportion of cells that tested positive for SAGE fluorescence indicated the initial events of SAGE uptake; and the GeoMean gave the average intracellular loads across the populations. These analyses corroborated the confocal imaging and revealed that a single positive charge on 50 % of the hub peptides is sufficient to maximize the efficiency of endocytosis. The addition of a single Glu residue did not alter uptake, but presentation of the E2 and E4 motifs reduced the internalization rate proportionally to the extension length. These effects on uptake are presumably due to the electrostatic interactions between the SAGE particle and the negatively charged cell membrane.

We also investigated the influence of tetralysine or tetraglutamate extensions at the *C* terminus of CC-Tri3 (Figure S14 & Table S3). These SAGE-K4^{488} and SAGE-E4^{488} particles were internalized at rates and resulted in intracellular distributions similar to their respective *N*-terminal analogues. Thus, overall charge on the SAGE particles is the discriminating factor rather than its precise placement within the peptide components.

Collectively, the uptake profiles of the *N*-terminally decorated SAGE compositions suggest that internalization rate can be controlled with surface charge. However, only a limited range of surface charges (and, consequently, uptake efficiencies) are accessible by extending charged residues from CC-Tri3. Therefore, we tested

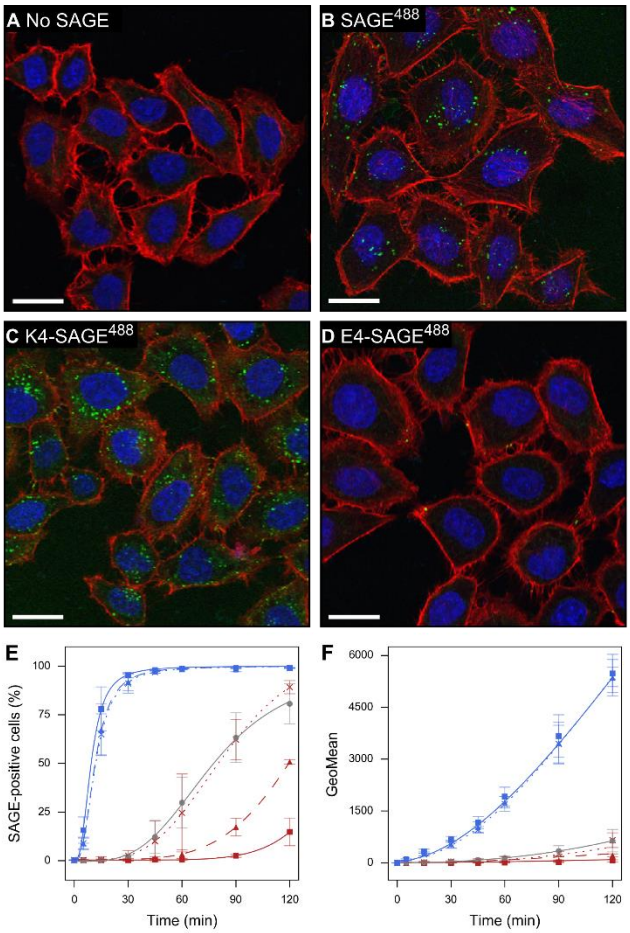

Figure 3. SAGE internalization by HeLa cells and the impact of surface electrostatics. (**A** – **D**) Representative confocal microscopy images of HeLa cells after 2 h exposure to no SAGE (**A**), SAGE^{488} (**B**), K4-SAGE^{488} (**C**) or E4-SAGE^{488} (**D**). SAGE particles are colored green and cells were labeled for F-actin (red; Alexa Fluor 594 Phalloidin) and nuclei (blue; DAPI). Scale bars: 10 μm. (**E** & **F**) Flow cytometry analysis of internalization of SAGE particles by HeLa cells, showing the percentage of cells counted as SAGE positive (**E**) and the population GeoMean (**F**). Key: SAGE^{488} (grey), K1-SAGE^{488} (blue; dotted, crosses), K2-SAGE^{488} (blue; dashed, triangles), K4-SAGE^{488} (blue; solid, squares) E1-SAGE^{488} (red; dotted, crosses), E2-SAGE^{488} (red; dashed, triangles), and E4-SAGE^{488} (red; solid, squares). Points show statistical mean ± standard deviation (n = 3).

if the modularity of the SAGE system could be exploited to more precisely control surface charge and tune the rate of endocytosis. To do this, we assembled four additional SAGE compositions carrying 12.5 or 25 % of K4-Hub-B or E4-Hub-B (Table S3). These compositions should carry the same surface charge as K1-, K2-, E1- and E2-SAGE^{488}, respectively, but in a different distribution across each particle. After a 2 h exposure, the four new compositions were found as puncta within HeLa cells by confocal microscopy with similar distributions to the respective one- and two-amino acid modified particles (Figure S15A – F). However, flow cytometry revealed clear differences in uptake between the two compositional preparations (Figure S15G & H), which are compared in Figure 4 and described as follows.

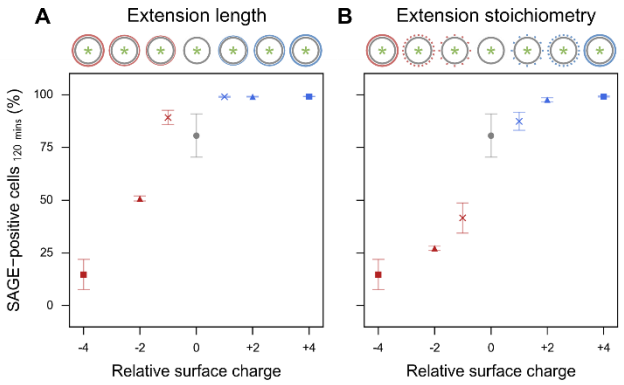

Figure 4. The degree of SAGE internalization can be tuned through surface electrostatics. The impact of relative SAGE surface charge on the proportion of SAGE-positive cells after 2 h when the charge is altered through extension length (A) and extension stoichiometry (B). Points show statistical mean ± standard deviation (n = 3). See Table S3 for full description of pictograms.

As stated above, the introduction of K1, K2 or K4 maximizes uptake, while the introduction of Glu residues reduces internalization proportionately to amount of introduced charge. However, when component stoichiometry is altered to control this charge, the endocytosis of SAGE particles is affected more subtly across the entire range of surface charges and therefore the efficiency of uptake can be more precisely selected. More specifically, altering surface charge through component stoichiometry provides finer control than through component alteration. This can be seen by comparing the shapes of the response to charge: when charge is altered by varying extension length, the plot effectively comprises two straight lines (Figure 4A); whereas, with the stoichiometric method the plot is more sigmoidal (Figure 4B).

In summary, we have shown that the component peptides and hubs of a *de novo* designed self-assembling peptide cage (SAGE) system can be embellished with linear peptide extensions and decorated by small molecules.[10b] These modifications do affect peptide structure and stability, but in predictable ways. The modified peptides can be incorporated into the hubs, which, in turn, assemble competently into SAGEs without affecting particle morphology. SAGE particles are endocytosed by mammalian cells and the efficiency of this uptake can be modulated by altering the electrostatic charge on the particle exterior: introducing positive charges enhances uptake, and negative charge reduces it. Altering surface charge by changing the stoichiometry of tetrapeptide-labelled variants brings more control to the system than modifying the component peptides with increasing numbers of charged residues. This highlights the value of modularity in self-assembly as employed in the SAGE system.[10b] By using this approach to control surface charge, the efficiency of internalization by mammalian cells is controlled in a manner hitherto unreported for other proteinaceous nanoparticle systems.[9a] Thus, this study lays the foundation for developing more-sophisticated SAGE and SAGE-like systems bearing functional decoration to provide cell-specific targeting and to port bioactive cargoes into cells. The endocytic pathways responsible for SAGE internalization are being investigated to explore further the potential of using SAGE particles to deliver such cargoes into cells and to traffic them within cells.

ASSOCIATED CONTENT

Supporting Information

Experimental details, peptide characterization and additional data. The Supporting Information is available free of charge on the ACS Publications website.

AUTHOR INFORMATION

Corresponding Authors

g.banting@bristol.ac.uk & d.n.woolfson@bristol.ac.uk

Author Contributions

‡J.L.B. and H.E.B. contributed equally.

Notes

The authors declare no competing financial interests.

ACKNOWLEDGMENTS

J.L.B. is supported by the BBSRC South West Doctoral Training Partnership. H.E.B. is funded by a BBSRC grant to G.S.B. and D.N.W. (BB/L010518/1). L.R.H. is funded by a BBSRC grant to P.V. and D.N.W. (BBM002969/1). D.N.W. is supported by grants from the BBSRC (BB/J008990/1) and ERC (340764). D.N.W. holds a Royal Society Wolfson Research Merit Award (WM140008). We would like to acknowledge BrisSynBio, a BBSRC/EPSRC-funded Synthetic Biology Research Centre, for use of their CEM Liberty Blue peptide synthesizer (BB/L01386X/1), the University of Bristol School of Chemistry Mass Spectrometry Facility for access to their EPSRC-funded Bruker Ultraflex MALDI TOF/TOF instrument (EP/K03927X/1), the Wolfson Bioimaging Facility (funded by the Medical Research Council and Wolfson Foundation) for access to their microscopy equipment and University of Bristol Faculty of Biomedical Sciences Flow Cytometry Facility for use of their BD FACSCanto II instrument.

REFERENCES

(1) Zhang, Y.; Chan, H. F.; Leong, K. W. *Adv. Drug Del. Rev.* **2013,** *65* (1), 104.

(2) (a) Couvreur, P. *Adv. Drug Del. Rev.* **2013,** *65* (1), 21; (b) Blanco, E.; Shen, H.; Ferrari, M. *Nat. Biotechnol.* **2015,** *33* (9), 941.

(3) Molino, N. M.; Wang, S.-W. *Curr. Opin. Biotechnol.* **2014,** *28* (1), 75.

(4) (a) Wörsdörfer, B.; Woycechowsky, K. J.; Hilvert, D. *Science* **2011,** *331* (6017), 589; (b) Sasaki, E.; Böhringer, D.; van de Waterbeemd, M.; Leibundgut, M.; Zschoche, R.; Heck, A. J. R.; Ban, N.; Hilvert, D. *Nat. Commun.* **2017,** *8* 14663; (c) Ardejani, M. S.; Chok, X. L.; Foo, C. J.; Orner, B. P. *Chem. Commun.* **2013,** *49* (34), 3528.

(5) (a) King, N. P.; Bale, J. B.; Sheffler, W.; McNamara, D. E.; Gonen, S.; Gonen, T.; Yeates, T. O.; Baker, D. *Nature* **2014,** *510* (7503), 103; (b) Bale, J. B.; Gonen, S.; Liu, Y.; Sheffler, W.; Ellis, D.; Thomas, C.; Cascio, D.; Yeates, T. O.; Gonen, T.; King, N. P.; Baker, D. *Science* **2016,** *353* (6297), 389; (c) Sciore, A.; Su, M.; Koldewey, P.; Eschweiler, J. D.; Diffley, K. A.; Linhares, B. M.; Ruotolo, B. T.; Bardwell, J. C. A.; Skiniotis, G.; Marsh, E. N. G. *Proc. Natl. Acad. Sci. U.S.A.* **2016,** *113* (31), 8681; (d) Kobayashi, N.; Yanase, K.; Sato, T.; Unzai, S.; Hecht, M. H.; Arai, R. *J. Am. Chem. Soc.* **2015,** *137* (35), 11285.

(6) (a) Doll, T. A. P. F.; Dey, R.; Burkhard, P. *J. Nanobiotechnology* **2015,** *13* (1), 73; (b) Gradišar, H.; Božič, S.; Doles, T.; Vengust, D.; Hafner-Bratkovič, I.; Mertelj, A.; Webb, B.; Šali, A.; Klavžar, S.; Jerala, R. *Nat. Chem. Biol.* **2013,** *9* (6), 362; (c) Ljubetič, A.; Lapenta, F.; Gradišar, H.; Drobnak, I.; Aupič, J.; Strmšek, Ž.; Lainšček, D.; Hafner-Bratkovič, I.; Majerle, A.; Krivec, N.; Benčina, M.; Pisanski, T.; Veličković, T. Ć.; Round, A.; Carazo, J. M.; Melero, R.; Jerala, R. *Nat. Biotechnol.* **2017,** *35* (11), 1094.

(7) Ljubetič, A.; Gradišar, H.; Jerala, R. *Curr. Opin. Chem. Biol.* **2017,** *40* (1), 65.

(8) Yeates, T. O.; Liu, Y.; Laniado, J. *Curr. Opin. Struct. Biol.* **2016,** *39* (1), 134.

(9) (a) Lee, E. J.; Lee, N. K.; Kim, I.-S. *Adv. Drug Del. Rev.* **2016,** *106* (1), 157; (b) Noble, J. E.; De Santis, E.; Ravi, J.; Lamarre, B.; Castelletto, V.; Mantell, J.; Ray, S.; Ryadnov, M. G. *J. Am. Chem. Soc.* **2016,** *138* (37), 12202; (c) Butterfield, G. L.; Lajoie, M. J.; Gustafson, H. H.; Sellers, D. L.;

Nattermann, U.; Ellis, D.; Bale, J. B.; Ke, S.; Lenz, G. H.; Yehdego, A.; Ravichandran, R.; Pun, S. H.; King, N. P.; Baker, D. *Nature* **2017,** *552* (7685), 415.

(10) (a) Fletcher, J. M.; Boyle, A. L.; Bruning, M.; Bartlett, G. J.; Vincent, T. L.; Zaccai, N. R.; Armstrong, C. T.; Bromley, E. H. C.; Booth, P. J.; Brady, R. L.; Thomson, A. R.; Woolfson, D. N. *ACS Synth. Biol.* **2012,** *1* (6), 240; (b) Fletcher, J. M.; Harniman, R. L.; Barnes, F. R. H.; Boyle, A. L.; Collins, A.; Mantell, J.; Sharp, T. H.; Antognozzi, M.; Booth, P. J.; Linden, N.; Miles, M. J.; Sessions, R. B.; Verkade, P.; Woolfson, D. N. *Science* **2013,** *340* (6132), 595.

(11) (a) Mosayebi, M.; Shoemark, D. K.; Fletcher, J. M.; Sessions, R. B.; Linden, N.; Woolfson, D. N.; Liverpool, T. B. *Proc. Natl. Acad. Sci. U.S.A.* **2017,** *114* (34), 9014; (b) Galloway, J. M.; Senior, L.; Fletcher, J. M.; Beesley, J. L.; Hodgson, L. R.; Harniman, R. L.; Mantell, J. M.; Coombs, J.; Rhys, G. G.; Xue, W.-F.; Mosayebi, M.; Linden, N.; Liverpool, T. B.; Curnow, P.; Verkade, P.; Woolfson, D. N. *ACS Nano* **2018,** *12* (2), 1420.

(12) Ross, J. F.; Bridges, A.; Fletcher, J. M.; Shoemark, D.; Alibhai, D.; Bray, H. E. V.; Beesley, J. L.; Dawson, W. M.; Hodgson, L. R.; Mantell, J.; Verkade, P.; Edge, C. M.; Sessions, R. B.; Tew, D.; Woolfson, D. N. *ACS Nano* **2017,** *11* (8), 7901.

(13) Albanese, A.; Tang, P. S.; Chan, W. C. W. *Annu. Rev. Biomed. Eng.* **2012,** *14* (1), 1.

(14) (a) Shoemaker, K. R.; Kim, P. S.; York, E. J.; Stewart, J. M.; Baldwin, R. L. *Nature* **1987,** *326* (6113), 563; (b) Doig, A. J.; Baldwin, R. L. *Protein Sci.* **1995,** *4* (7), 1325; (c) Baker, E. G.; Bartlett, G. J.; Crump, M. P.; Sessions, R. B.; Linden, N.; Faul, C. F. J.; Woolfson, D. N. *Nat. Chem. Biol.* **2015,** *11* (3), 221.

(15) Huotari, J.; Helenius, A. *EMBO J.* **2011,** *30* (17), 3481.

Authors are required to submit a graphic entry for the Table of Contents (TOC) that, in conjunction with the manuscript title, should give the reader a representative idea of one of the following: A key structure, reaction, equation, concept, or theorem, etc., that is discussed in the manuscript. Consult the journal's Instructions for Authors for TOC graphic specifications.

Insert Table of Contents artwork here